ISSN 2047-0371

3.2.3. Surf Zone Hydrodynamics: Measuring Waves & Currents

Kris W. Inch[1]
[1] Coastal Processes Research Group, School of Marine Science and Engineering, University of Plymouth (kris.inch@plymouth.ac.uk)

ABSTRACT: Wave breaking is the most significant energy input into wave-dominated coastal environments and is responsible for driving a number of interrelated, hydrodynamic processes in a region known as the surf zone. Surf zone hydrodynamics occur over a range of spatial and temporal scales and are constantly changing. As a result, obtaining measurements of waves and currents in the surf zone can be challenging and field experiments require detailed planning to ensure the collection of useful data. Measurements of surf zone hydrodynamics are divided into two general categories: (1) non-directional wave measurements; and (2) directional wave and current measurements. Near-bed pressure transducers are by far the most common method of measuring the non-directional properties of waves. Acoustic sensors are being used with increasing frequency for Eulerian measurements of surf zone currents, whereas Lagrangian surf zone drifters are most useful for measuring flow patterns in rip currents, surf zone circulation and alongshore currents. This article gives a summary of the various methods of measuring waves and currents in the surf zone. Additionally, simple data analysis techniques to study infragravity waves are demonstrated.

KEYWORDS: surf zone, breaking waves, pressure transducer, current meters, infragravity waves.

Introduction

The surf zone is that part of the shoreface extending from the seaward boundary of wave breaking to the swash zone; the part of the beach that is alternately covered and exposed by wave uprush and backwash. Breaking waves drive a number of interrelated surf zone processes such as the creation of turbulent bores, wave set-up, nearshore currents and low frequency motions. Together these processes force the entrainment and transport of sediment, which leads to morphological change. For a comprehensive overview of surf zone processes see Komar (1998), or the introductory texts of Aagaard and Masselink (1999), Woodroffe (2002), Davidson-Arnott (2010) and Masselink *et al*. (2011) for a more succinct summary.

The width and characteristics of the surf zone vary constantly, driven by changes in the tide elevation, incident wave height and direction, low-frequency motions and local wind speed. The beach slope also plays an important role in determining the breaker type and dissipative characteristics of the surf zone. Three types of breaking waves are commonly recognised (Figure 1); spilling, plunging and surging (Galvin, 1968). Spilling waves typically occur on low gradient beaches and dissipate their energy gradually over a wide surf zone. With plunging breakers, the shoreward face of the wave steepens until it is vertical and the crest curls over and plunges forward and downward as an intact mass of water. Plunging waves are more energetic than spilling waves at the point of breaking and are normally associated with narrower surf zones and steeper beaches. Surging waves are found on steep, reflective beaches where there is often no clear surf zone as the waves slide up the beach without physically breaking. In reality, there is a continuum of breaker types blending from one to another and on a natural beach with a spectrum of wave heights and periods it is common to see a range of breaker types at a given time. A number of dimensionless parameters have been developed to predict

the breaker type and surf zone state. The most widely used of these is the Iribarren number ξ defined as

$$\xi = \frac{tan\beta}{\sqrt{H_b/L_o}}$$

where β is the beach slope, H_b is the breaker height and L_o is the deep water wavelength given by linear wave theory. Spilling waves occur when ξ < 0.4, plunging waves occur when 0.4 < ξ < 2.0, and surging waves occur when ξ > 2.0 (Battjes, 1974).

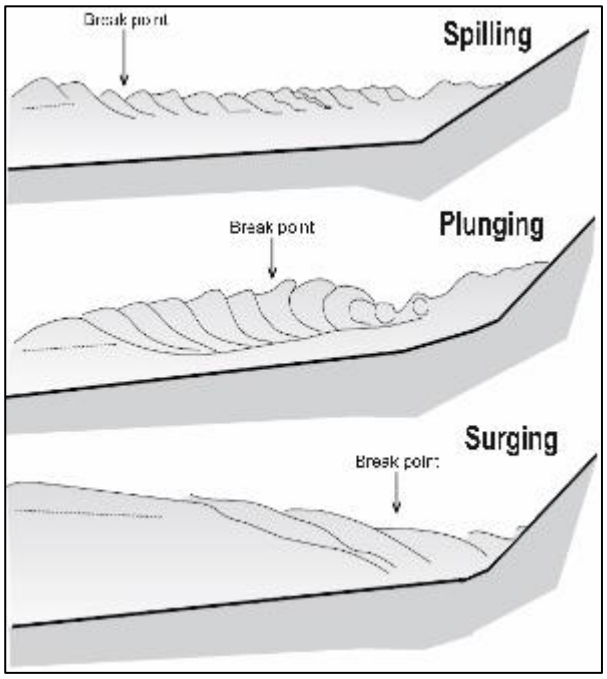

Figure 1: The three types of breaking wave. Note the different break point locations in relation to the shoreline. Modified from Davidson-Arnott (2010).

In the inner surf zone of low gradient, dissipative beaches, the incident wave height H is controlled by the local water depth (Thornton and Guza, 1982) and can be expressed by

$$H = \langle\gamma\rangle h$$

where γ is a coefficient ranging from 0.3-0.6 and increases with beach slope, and h is water depth. When the wave height is limited by the local water depth the surf zone is considered to be saturated. Under saturated conditions, to maintain a constant relationship between wave height and water depth, an increase in offshore wave height acts only to increase the width of the surf zone. However, on steep, sandy beaches plunging waves break close to shore creating a narrow surf zone that can remain unsaturated.

The inner surf zone is of particular importance as the conditions here force the hydro and sediment dynamics in the swash zone, which is arguably the most dynamic part of the nearshore region (Masselink and Puleo, 2006). Water motion in the inner surf zone is typically dominated by infragravity waves, particularly on dissipative beaches. Infragravity waves are low-frequency (0.005-0.05 Hz) waves that approach the shoreline bound to incident wave groups but become free waves in the surf zone following incident wave breaking. Infragravity waves are an important research topic for coastal scientists as they play an important role in beach and dune erosion, especially during storms (Russell, 1993). Due to their long wavelengths, which prevent breaking, infragravity waves reflect from the shoreline and travel seawards giving rise to a cross-shore quasi-standing wave pattern (Guza and Thornton, 1985). Infragravity energy in the surf zone increases with increasing offshore wave height; however, recent studies have revealed that under very energetic wave conditions infragravity waves may also become saturated (e.g. Senechal *et al*., 2011a; Guedes *et al*., 2013; De Bakker *et al*., 2014).

In addition to wave motion, three types of quasi-steady, wave-induced currents exist in the surf zone; bed return flow, alongshore currents and rip currents. These currents exist simultaneously and are driven by cross-shore and alongshore gradients in the mean water level caused by variations in the wave breaker height. The intensity of nearshore currents increases with increasing incident wave height. Thus, the strongest currents capable of transporting vast quantities of sediment occur during storms (Senechal *et al*., 2011b). Additionally, rip currents pose a significant hazard to water users and are a major cause of lifeguard rescues around the world (Short and Brander, 1999; Scott *et al*., 2007, 2008).

Measurements of surf zone processes are of vital importance for estimating potential storm damage, modelling shoreline evolution and designing shoreline management plans. Waves and currents are well documented in the coastal literature; advances in instrument

technology and analysis techniques have improved our knowledge considerably over the last few decades. However, certain aspects remain poorly understood, such as surf zone hydrodynamics during extreme storms. The purpose of this entry is to provide an overview of the current *in situ* methods of measuring surf zone waves and currents, and to give a simple demonstration of wave data analysis.

Surf Zone Measurements

For convenience, the following section on surf zone measurements is split into two main categories: (1) non-directional wave measurement; and (2) directional wave and current measurement. Non-directional wave measurements are measurements of the water surface elevation from which information about wave height and period can be obtained. Current measurements are measurements of the velocity vector and are used to study nearshore currents and the directional properties of waves.

Non-directional wave measurement

Field measurements of waves have previously been collected using a form of surface piercing wave staff (among others, Thornton and Guza, 1983; Davidson-Arnott and McDonald, 1989). Wave staffs are part of an electronic circuit that takes advantage of the conductivity of sea water by recording the change in electrical resistance or capacitance as waves pass the instrument. These recordings are then converted to measurements of water depth using calibrated signals from known water depths. The sensors can be attached to a temporary support driven into the sand or attached to a more permanent structure such as a pier. The advantage of using wave staffs is that they provide a direct measure of the sea surface elevation. The main disadvantage of wave staffs is that they are exposed to wave action when deployed in shallow water or in energetic surf zones. This can damage wave staffs or displace them from their intended vertical positions, thus causing error in the water depth measurements. Furthermore, mounting requirements restrict the use of wave staffs at certain locations and may limit the deployment of additional sensors at the same location.

Nowadays, almost all surf zone field experiments use bottom-mounted pressure transducers. Pressure transducers measure pressure variations associated with passing waves above and this pressure is converted (either by the sensor or in post-processing) into the equivalent water depth. Pressure transducers are most commonly attached to a temporary frame driven into the sand (Figure 2a), but can also be fixed to permanent features such as shore platforms or buried beneath the surface of the beach. An advantage of using buried pressure transducers is to avoid corruption of the signal caused by dynamic pressure variations from accelerating and decelerating flows (Austin *et al*., 2014). Unlike wave staffs, pressure transducers are not directly exposed to wave action. They are also relatively easy to deploy, can be co-located with other sensors and are often self-logging eliminating the need for cables.

The main limitation of using pressure transducers is depth attenuation of the pressure signal. The extent of depth attenuation is frequency dependant; as depth increases high frequency signals are lost before low frequency signals. Depth attenuation can be corrected for during post-processing by applying a frequency dependant depth attenuation factor $K(f)$ derived from linear wave theory as:

$$K(f) = \frac{\cosh(kz)}{\cosh(kh)}$$

where k is the frequency dependant wave number ($2\pi/L$, where L is wavelength) and z is the height of the pressure sensor above the bed. A consequence of using this method to correct for depth attenuation is that it introduces high frequency noise, which can cause significant error at the data analysis stage. Therefore a high frequency cut-off should be chosen beyond which energy in the wave spectrum (see *Wave Data Analysis*) is discarded. The high frequency cut-off should be chosen carefully depending on factors such as the sensor depth and local wave climate. However, an alternative method of determining the high frequency cut-off ω_c is by

$$\omega_c = 0.564\pi\sqrt{(g/d)}$$

(Green, 1999; Aagaard *et al*., 2002) where ω is radian frequency ($2\pi f$, where f is frequency), g is gravitational acceleration

(9.81 m s^{-2}) and d is the depth of the pressure sensor. Pressure transducers deployed in the surf zone tend to be located in relatively shallow water compared to open ocean deployments. Nonetheless, correcting for depth attenuation is an important process, especially in macrotidal regions and low fetch environments where high frequency wind waves prevail. In addition to depth attenuation, there is also the need to correct for atmospheric pressure. Some pressure transducers do this automatically using the mean atmospheric pressure at sea level (10.1325 dbar); however, this does not account for local variations in atmospheric pressure or short term fluctuations during an experiment, for which local pressure observations are required.

An additional source of error in water depth measurements provided by pressure transducers arises from the unknown height of the sensor above the bed. If this offset is measured at the start of an experiment and at every opportunity thereafter, a linear function may be used to correct for bed level change between measurements. However, the results of recent studies in the inner surf zone (e.g. Puleo *et al*., 2014) suggest that net bed level change over a tidal cycle may not be linear but rather the result of just a few "large" waves. A way to overcome this is by co-locating the pressure transducer with a sensor, such as an ultrasonic distance meter, providing continuous measurements of bed level elevation (e.g. Ridd, 1992; Saulter *et al*., 2003; Arnaud *et al*., 2009; Puleo *et al*., 2010; *et al*., 2014). Whilst the unknown height of the pressure transducer can cause error in measurements of total water depth, Ruessink (1999) suggests that the impact of these uncertainties on wave height calculations is < 10%.

Directional wave and current measurement

Wave staffs and pressure transducers provide a time series of the water surface elevation, which is useful for studying wave height and period. However, in order to investigate directional wave properties and nearshore currents, the horizontal component of water motion also needs to be measured. Current data can broadly be divided into two categories: (1) Eulerian observations; and (2) Lagrangian observations. Eulerian methods measure fluid flow at a fixed location through time, whereas Lagrangian methods follow fluid parcels through space and time. Eulerian observations are collected by *in situ* current meters, often co-located with pressure transducers and referred to as PUV set-ups (Figure 2b) due to the three quantities measured; pressure (*P*) with cross-shore (*U*) and alongshore (*V*) velocities (Morang *et al*., 1997).

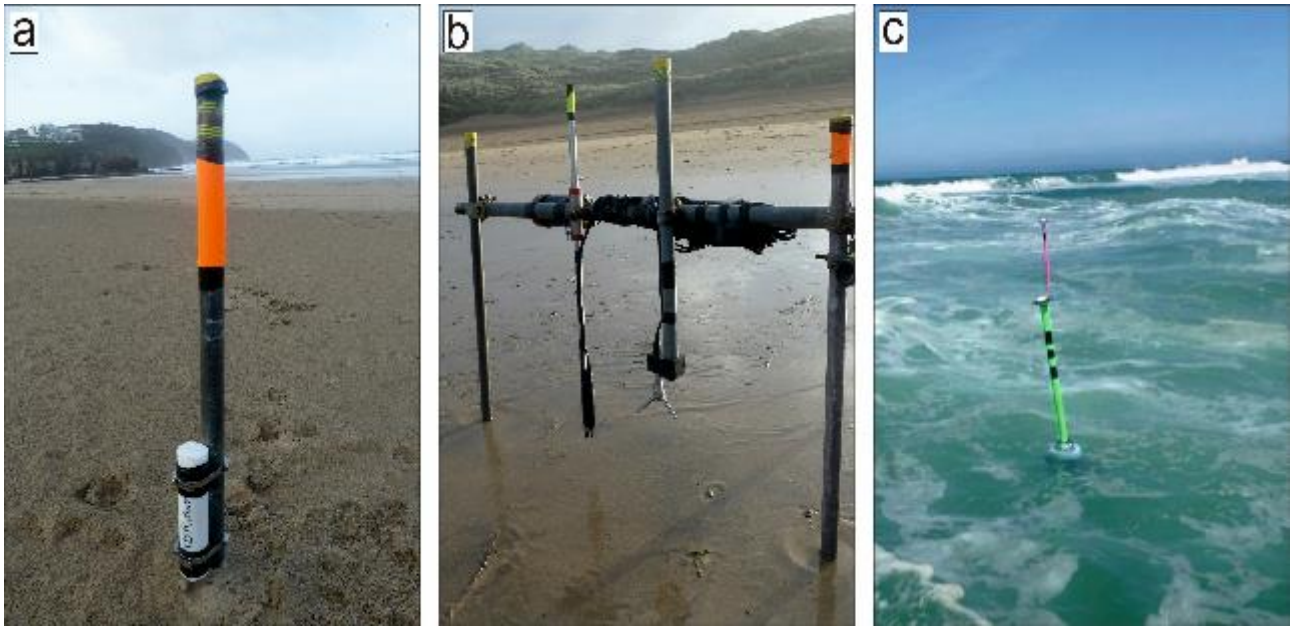

Figure 2: Examples of (a) a bottom-mounted pressure transducer, (b) a PUV rig equipped with an acoustic Doppler velocimeter, and (c) surf zone drifters. (Photos: K. Inch and E. Woodward)

These types of measurements are useful for studying directional wave properties and near-bed currents. Lagrangian observations are most useful in studies of rip currents, surf zone circulation and surf zone flushing where current magnitude and direction vary spatially in the surf zone.

Eulerian observations

Since their introduction in the 1970s, electromagnetic current meters (EMCMs) have been widely used to measure currents in the surf zone. EMCMs measure the voltage generated by waves passing through a fluctuating magnetic field produced by the sensor. Faraday's law is then used to convert the voltage into the proportional current velocity along two perpendicular axes (*u*,*v*). Over the past decade or so, acoustic Doppler velocimeters (ADVs) have become a popular alternative to EMCMs. ADVs operate by emitting acoustic signals into the water column and recording the return signal backscattered by fine material a short distance from the sensor. Current velocity is calculated using the phase lag between successive return signals. ADVs are seen as an advancement on EMCMs as they measure three-dimensional (*u*,*v*,*w*) velocity components and are non-intrusive (MacVicar *et al*., 2007). Also, EMCMs are prone to error if the sensor is located too close to the seabed or free surface, drift of the zero offset and electronic interference (Guza *et al*., 1988). A significant problem with using ADVs in the surf zone, however, is their high sensitivity to bubbles and sediment which results in poor data (determined by the signal to noise ratio) being removed in quality control procedures (Elgar *et al*., 2005; Feddersen, 2010). The lower sensitivity of EMCMs means that they remain a practical and much used instrument in surf zone studies and, under highly turbulent conditions, may outperform ADVs (e.g. Rodriguez *et al*., 1999). Elgar *et al*. (2001) simultaneously deployed EMCMs and ADVs on the same frame in the surf zone to provide a direct and detailed comparison of their performance. They found that the data were highly correlated in velocities up to 3 m s^{-1}, confirming the ability of both instruments to perform well at measuring surf zone currents.

There has been increasing interest in recent years in using pulse-coherent acoustic Doppler profilers (ADPs) to monitor surf zone hydrodynamics (e.g. Senechal *et al*., 2011b). ADPs operate using the same basic principles as ADVs and are therefore also highly sensitive to bubbles and sediment. However, by measuring the return signal in much smaller time increments, ADPs determine the velocity vector for a series of discrete "bins" over a portion of the water column. This makes ADPs especially useful for studying boundary layer dynamics in the surf zone. For example, Puleo *et al*. (2012) used an ADP to investigate the inner surf zone boundary layer at a spatial resolution of 1 mm and a temporal resolution of 100 Hz on a microtidal beach in Florida, USA.

Lagrangian observations

A Lagrangian method which is particularly popular in Australian research is releasing a bright, inert dye into the surf zone and tracking its movement (e.g. Huntley *et al*., 1988; Brander, 1999; Brander and Short, 2001). Dye tracking is useful in providing qualitative data on the location and path of nearshore currents and is a valuable tool in beach safety education. However, it does not provide any data on actual current velocities. An increasingly popular technique for measuring the flow patterns in nearshore currents is using GPS-tracked surf zone drifters (Figure 2c). Surf zone drifters are buoyant, PVC tubes equipped with on-board GPS data loggers which record the drifter's position in the surf zone at typically 0.5-1 Hz (Schmidt *et al*., 2003). The drifters are equipped with a damping plate designed to allow broken waves to pass without rapidly transporting the drifter onshore (Schmidt *et al*., 2003). Accuracies of < 0.4 m in position and < 0.01 m s^{-1} in velocity can be achieved by post-processing the raw GPS data from a static base position (MacMahan *et al*., 2009). The combined tracks of multiple drifters provide detailed information on mean nearshore flow patterns and velocities (e.g. Austin *et al*., 2010, 2014). Surf zone drifters have been observed to closely follow simultaneous dye releases as well as provide velocity measurements in good agreement with those from *in situ* current meters, thus confirming their ability to make valid Lagrangian observations of surf zone currents (Schmidt *et al*., 2003; Johnson and Pattiaratchi, 2004; MacMahan *et al*., 2009). A recent study by McCarroll *et al*. (2014) used

34 surf zone drifters to investigate rip current behaviour on an embayed beach in New South Wales, Australia. They were able to make 293 individual drifter deployments over a single ebbing tidal cycle, thus providing a detailed observation of the nearshore flow patterns (Figure 3).

Remote sensing

It is beyond the scope of this entry to discuss remote sensing methods in detail; however, it should be acknowledged that remote sensing techniques are being used with increasing frequency to study nearshore waves and currents (for a review, see Holman and Haller, 2013). These methods include video imagery (e.g. Holman *et al*., 2006; Holman and Stanley, 2007; De Vries *et al*., 2011), X-band radar (e.g. Ruessink *et al*., 2002; Catalan *et al*., 2014; Haller *et al*., 2014) and LIDAR (e.g. Blenkinsopp *et al*., 2012). Possible advantages of using remote sensing methods include better synoptic measurements, lower maintenance costs, improved robustness and longer deployments including during storms. A potential disadvantage of remote sensing is that measurements are often based on a proxy rather than a direct measurement; therefore, the accuracy of the measurements depends on how well the proxy represents the variable being studied.

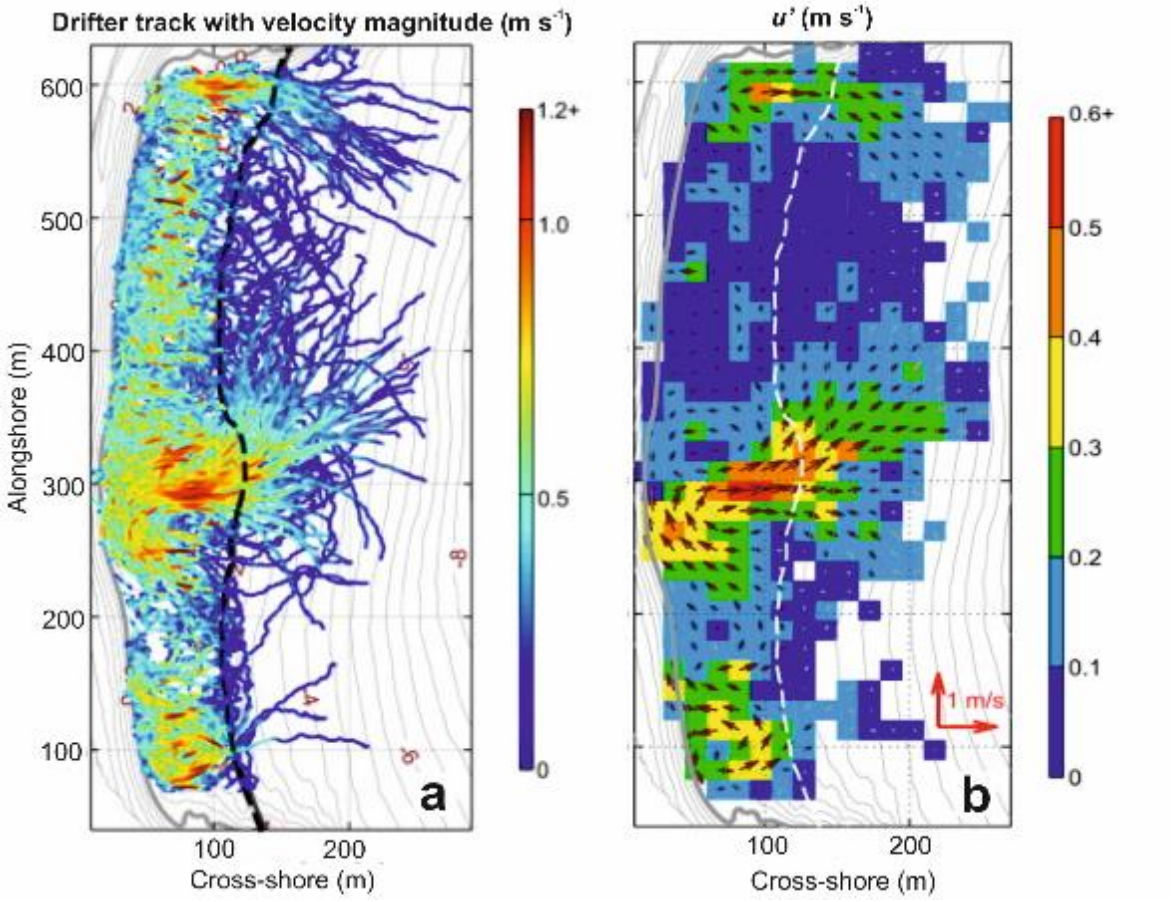

Figure 3: Drifter tracks coloured by velocity magnitude (a), and mean velocity magnitude and direction determined from individual drifter observations (b). Contours are at 0.5 m spacing and the edge of the surf zone is indicated by the black dashed line in (a) and white dashed line in (b). (Source: McCarroll et al., 2014)

Wave Data Analysis

The analysis of surf zone data is very complex and it is far beyond the scope of this article to discuss all types of analysis techniques. The most appropriate analysis procedure depends on the aim of the research and the type of data available. In this section, the analysis of wave and current data to investigate infragravity waves in the surf zone (see *Introduction*) is discussed as an example. Data collected from the inner surf zone of Perranporth Beach, Cornwall, UK, is used to demonstrate the analysis

techniques. Perranporth is a macrotidal, dissipative beach with a mean tidal range of 5.4 m and is composed of medium sand. Observations of pressure and velocity (*u*,*v*,*w*) were logged continuously at 4 Hz using a co-located pressure transducer and ADV during a large storm in October 2013. The instruments were mounted onto a temporary scaffold frame driven into the sand in the intertidal zone (Figure 2b). The height of the instruments above the bed was measured before and after each tide and a linear function was used to correct for changes in bed level. The pressure data were converted to water surface elevation, with a depth correction using linear wave theory and a high frequency cut-off of 1 Hz (see *Surf Zone Measurements*), and detrended prior to analysis.

There are generally two approaches to analysing wave data; analysis in the time domain and in the frequency domain.

Time domain analysis

The irregular nature of natural waves is evident in the example time series of water surface elevation and cross-shore velocity shown in Figure 4a and 4b. The two time series have limited value in their raw state and are best described quantitatively using statistics. The two most common statistical parameters used to describe a wave time series are the significant wave height H_s (also $H_{1/3}$) which is the mean of the highest one third of waves, and the peak wave period T_p which is the wave period associated with the maximum wave energy derived from the wave spectrum (described below). Other commonly used wave parameters include the mean wave height $\overline{H}$, maximum wave height H_{max} and zero-crossing wave period T_z. A summary of the various wave parameters that can be derived from both time and frequency domain analysis is given by Morang *et al*. (1997).

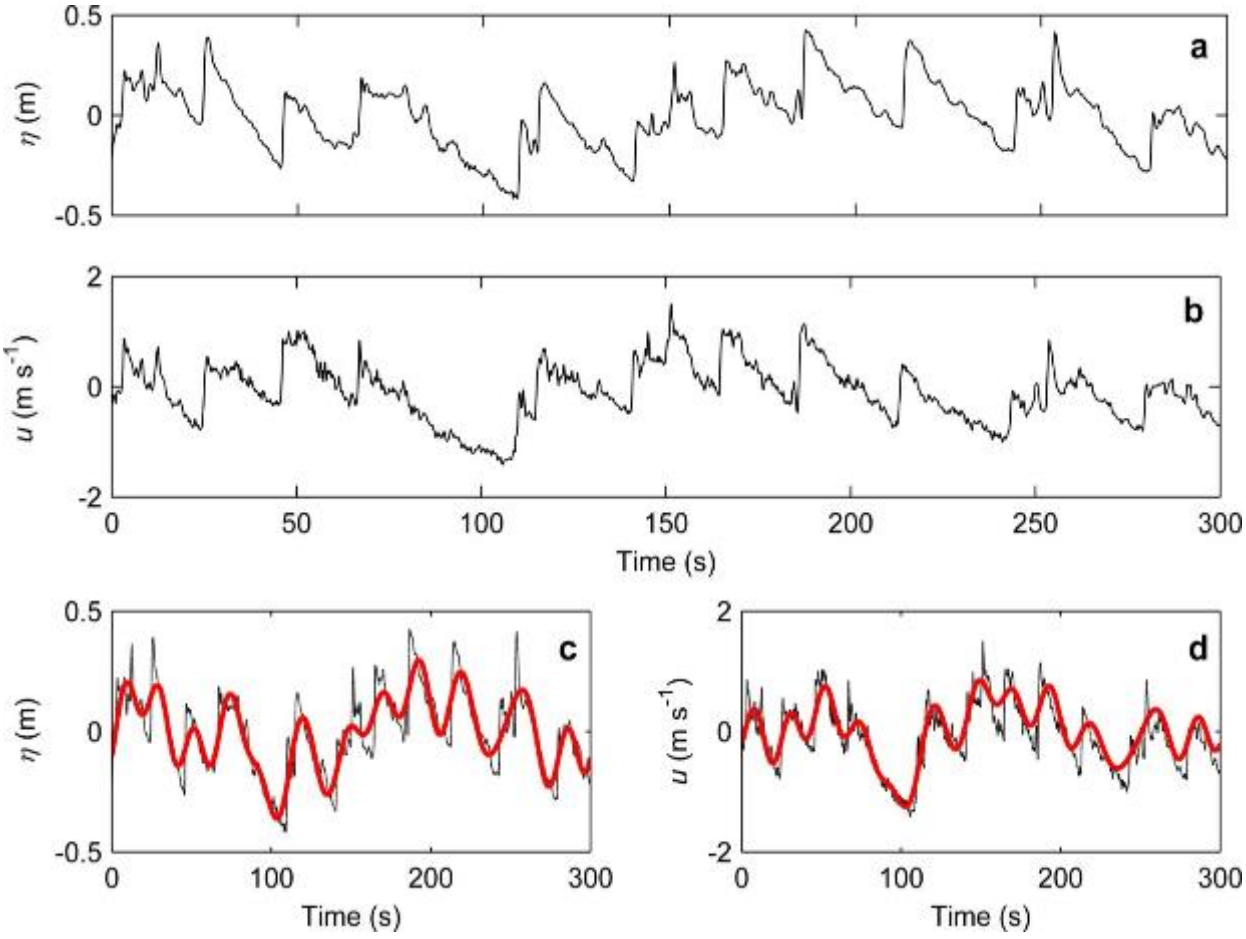

Figure 4: Raw time series (5 mins) of water surface elevation η (a) and cross-shore velocity u (b) collected in the inner surf zone of Perranporth Beach during storm conditions with an offshore significant wave height of 4.31 m. Low pass filtered (0.005-0.05 Hz) water surface elevation (c) and cross-shore velocity (d) time series (red) plotted with the original time series (black).

One method to obtain these wave parameters is through wave-by-wave analysis using the zero-downcrossing method. The zero-downcrossing method defines an individual wave by two successive downward crossings of the mean water level by the water surface elevation. Alternatively, Longuet-Higgins (1952) proposed a method based on the Rayleigh distribution, which calculates the various wave height parameters using the standard deviation of the water surface elevation time series. Significant wave height, for example, can be estimated from

$$H_s = 4\sigma_\eta$$

where σ_η is the standard deviation of the water surface elevation. To calculate wave statistics over particular frequency ranges (e.g. infragravity and incident), high- and low-pass filters can be applied to the original time series. Figure 4c and 4d shows the filtered infragravity components plotted with the original time series from Figure 4a and 4b. The infragravity time series follow closely the original time series for both water surface elevation and cross-shore velocity. This is a clear indication that the dominant water motion is at infragravity frequencies and the calculated significant wave heights reflect this; 0.58 m and 0.30 m for the infragravity and incident bands respectively. This is typical of water motion in the inner surf zone of dissipative beaches.

As mentioned in the introduction, the long wavelengths of infragravity waves inhibit wave breaking allowing some energy to reflect from the shoreline. Therefore, the low frequency signal of a wave time series will comprise both incoming (shoreward) and outgoing (seaward) components. Guza *et al*. (1984) proposed a method to decompose the shoreward and seaward propagating wave signals in the time domain using the water surface elevation and cross-shore velocity by:

$$\eta_{in} = \frac{\eta + \sqrt{h/g}\,u}{2}$$

$$\eta_{out} = \frac{\eta - \sqrt{h/g}\,u}{2}$$

where η_{in} and η_{out} are the incoming and outgoing wave components, η is water surface elevation and u is cross-shore velocity. This method was used to separate the infragravity wave signal in Figure 4c into its incoming and outgoing components and corresponding significant wave heights were calculated. The significant wave height of the outgoing infragravity time series was 0.23 m, indicating that some wave energy was indeed reflected. It is also possible to separate the incoming and outgoing wave components in the frequency domain (discussed below).

Frequency domain analysis

Wave data analysis in the frequency domain is achieved through spectral analysis. Spectral analysis is based on the fast Fourier transformation, which assumes that a time series is composed of a finite number of sinusoids at discrete frequencies. Spectral analysis partitions a time series into its constituent parts and produces an auto-spectrum (sometimes referred to as a wave spectrum); a plot of wave variance (proportional to wave energy) as a function of frequency. An outline and worked example of the various steps involved to produce a wave spectrum is given by Hegge and Masselink (1996). Figure 5a-c shows the water surface elevation, cross-shore and alongshore velocity auto-spectra of an extended version of the time series in Figure 4. The auto-spectra reveal that most of the variance in water surface elevation and cross-shore velocity is at infragravity frequencies; 87.7% and 88.4% respectively. The alongshore velocity auto-spectrum, however, shows less variance over a broader range of frequencies.

An extension of spectral analysis that is useful in the study of infragravity waves is cross-spectral analysis. Cross-spectral analysis is used to determine the level of co-variance and phase lag between two time series (Jenkins and Watts, 1968). If the cross-shore structure of infragravity waves is standing, cross-spectral analysis will reveal a phase difference of 90° (π/2) between the water surface elevation and cross-shore velocity (Suhayda, 1974). Cross-spectral analysis has also been used to investigate the relationship between infragravity waves and wave groups in the surf zone (e.g. Masselink, 1995).

The decomposition of wave energy into incoming and outgoing components in the frequency domain can be achieved in two ways; (1) using pressure and cross-shore velocity measurements from co-located

sensors, or (2) using pressure measurements only from a cross-shore array of pressure transducers. The method of Sheremet *et al*. (2002) is an example of the first technique where the incoming and outgoing energy E at each discrete frequency is calculated as:

$$E^{\pm}(f) = \frac{1}{4}\left[S_p(f) + \frac{h}{g}S_u(f) \pm \left(2\sqrt{\frac{h}{g}}\right)C_{pu}(f)\right]$$

where S_p and S_u are the pressure and cross-shore velocity auto-spectra respectively and C_{pu} is the $p-u$ cospectrum. The second technique uses calculations of wave celerity and phase lag as waves travel through an array of normally three or more pressures transducers. A number of solutions exist that employ this method such as those of Gaillard *et al*. (1980), Battjes *et al*. (2004) and Van Dongeren *et al*. (2007). The type of decomposition method used will largely depend on instrument availability and the overall aim of the study. De Bakker *et al*. (2014) performed a comparison between the $p-u$ method of Sheremet *et al*. (2002) and the array method of Van Dongeren *et al*. (2007) using data collected in the surf zone of a dissipative beach in the Netherlands and found relatively good agreement between the two methods.

Following the decomposition of wave energy by one of the above methods, frequency dependant (and bulk) reflection coefficients $R^2(f)$ can be calculated which are simply the ratio of seaward to shoreward propagating wave energy flux $F^{\pm}(f)$ (calculated as $E^{\pm}(f)\sqrt{gh}$).

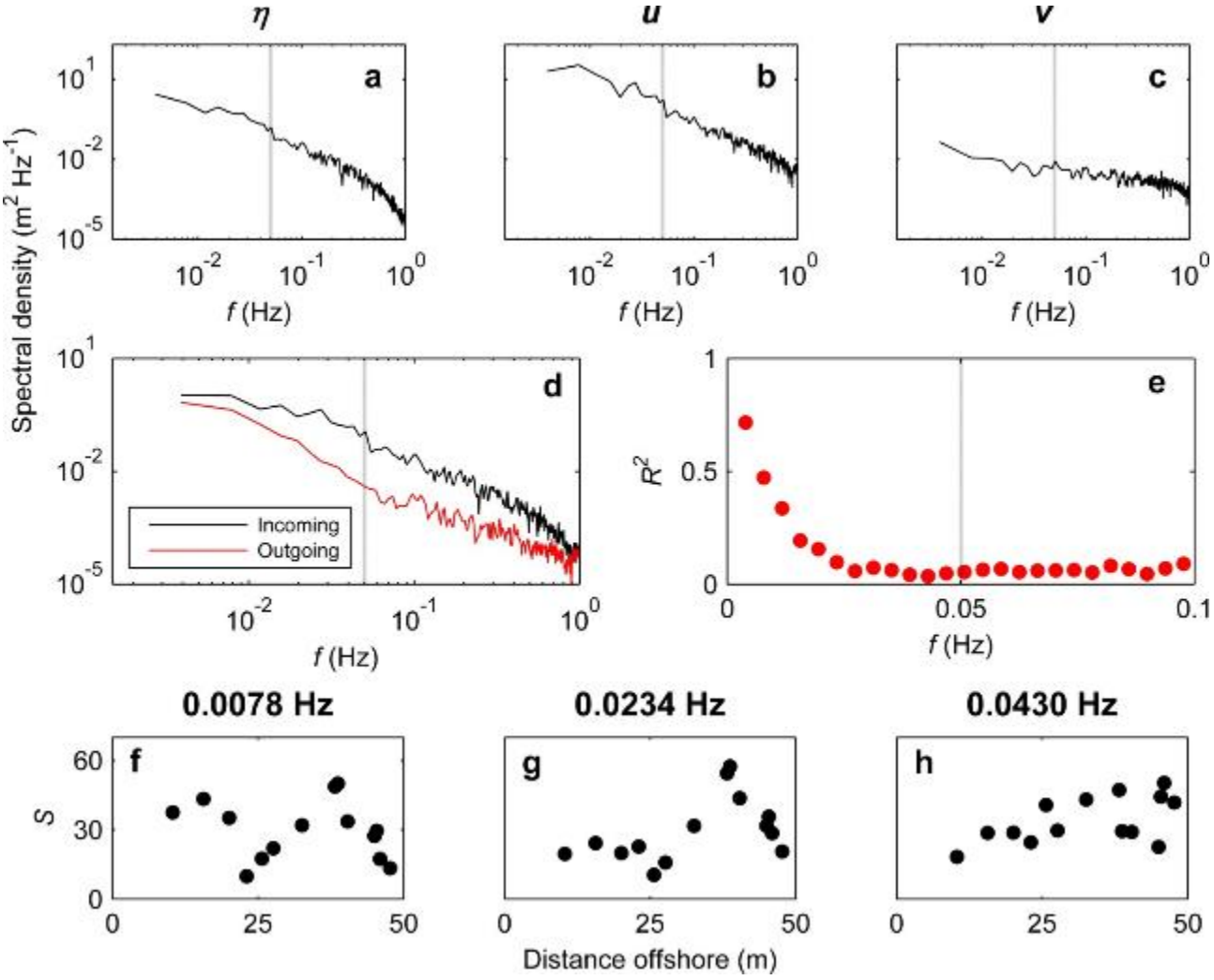

Figure 5: Auto-spectra of water surface elevation η (a), cross-shore velocity u (b) and alongshore velocity v (c). Incoming and outgoing water surface elevation auto-spectra (d) using the separation method of Sheremet et al. (2002) and corresponding reflection coefficients R^2 (e). Normalised spectral density S versus distance offshore for three infragravity frequencies (f-h). Vertical dotted lines in a-e indicate the infragravity-incident frequency transition of 0.05 Hz.

Figure 5e shows the frequency dependant reflection coefficients corresponding to the incoming and outgoing spectra in Figure 5d (estimated using the method of Sheremet *et al*. (2002) outlined above). The reflection coefficients show that only frequencies at the lower end of the infragravity band reflect a significant amount of energy; R^2 is less than 0.1 for all frequencies higher than 0.0273 Hz indicative of > 90% energy dissipation.

To gain a detailed insight into the cross-shore structure and transformation of infragravity (and incident) waves, the techniques described above can be applied to data collected at a number of cross-shore locations. This can be achieved through the deployment of an instrument array, or deploying a single instrument rig and using the tide as a surrogate for changing cross-shore position. The latter option requires fewer instruments, but is limited to sites with a large tidal range, linear beach profile and no change in forcing conditions during the study. The cross-shore structure of energy at three discrete frequencies in the infragravity band is demonstrated in Figure 5f-h by plotting the spectral density at these frequencies versus distance offshore. In this example the tide was used as a proxy for changing cross-shore position, hence the spectral density is normalised by the offshore wave height. It can be seen that at 0.0078 Hz there is a clear (anti)nodal structure symbolic of standing waves with antinodes at 15 m and 40 m and a node at 24 m. This is partially lost at 0.0234 Hz and completely absent at 0.0430 Hz which displays a progressive wave pattern. This agrees well with the reflection coefficients in Figure 5e.

Concluding Remarks

The surf zone is highly energetic and can be a challenging environment in which to collect wave and current measurements. The data, however, are invaluable and there have been many advances in instrument technology over the last few decades, which have helped to further our knowledge of surf zone hydrodynamics. Pressure transducers are undeniably the most commonly used and arguably the most valuable device for measuring waves. There has been a shift towards the use of acoustic sensors for measuring surf zone currents, yet EMCMs remain a valuable tool, especially during turbulent conditions.

Detailed planning, including a thorough understanding of the various sensors and analysis procedures, is crucial to ensure the collection of a high quality, useful dataset. There are several important considerations that need to be included such as the local wave climate, sampling strategy, data retrieval and analysis techniques, and the overall aim of the research. Researchers are advised to review the relevant literature before undertaking a field experiment in order to achieve the optimal set-up for their project.

Acknowledgements

The comments and suggestions of two anonymous reviewers helped to improve the clarity of this article. The author also thanks Dr Mark Davidson and Prof. Paul Russell for their constructive feedback on an early draft. Fieldwork assistance at Perranporth was provided by Dr Mark Davidson, Prof. Paul Russell, Dr Tim Scott and Mr Luis Melo de Almeida.

References

Aagaard T, Masselink G. 1999. The Surf Zone. In *Handbook of Beach and Shoreface Morphodynamcis*, Short AD (ed.). Wiley: Chichester; 72-118.

Aagaard T, Black KP, Greenwood B. 2002. Cross-shore suspended sediment transport in the surf zone: a field-based parameterization. *Marine Geology* **185**: 283-302.

Arnaud G, Mory M, Abadie S, Cassen M. 2009. Use of a resistive rods network to monitor bathymetric evolution in the surf/swash zone. *Journal of Coastal Research* **SI 56**: 1781-1785.

Austin M, Scott T, Brown J, Brown J, MacMahan J, Masselink G, Russell P. 2010. Temporal observations of rip current circulation on a macro-tidal beach. *Continental Shelf Research* **30**: 1149-1165.

Austin MJ, Masselink G, Scott TM, Russell PE. 2014. Water-level controls on macro-tidal rip currents. *Continental Shelf Research* **75**: 28-40.

Battjes JA. 1974. Surf similarity. *Proceedings of the 14th Coastal Engineering Conference*, ASCE, 466-480.

Battjes JA, Bakkenes HJ, Janssen TT, Van Dongeren AR. 2004. Shoaling of subharmonic gravity waves. *Journal of Geophysical Research* **109**: C02009.

Blenkinsopp CE, Turner IL, Allis MJ, Peirson WL, Garden LE. 2012. Application of LIDAR technology for measurement of time-varying free-surface profiles in a laboratory wave flume. *Coastal Engineering* **68**: 1-5.

Brander RW. 1999. Field observations on the morphodynamic evolution of a low-energy rip current system. *Marine Geology* **157**: 199-217.

Brander RW, Short AD. 2001. Flow Kinematics of Low-energy Rip Current Systems. *Journal of Coastal Research* **17**: 468-481.

Catalan PA, Haller MC, Plant WJ. 2014. Microwave backscattering from surf zone waves. *Journal of Geophysical Research* **119**: 3098-3120.

Davidson-Arnott RGD, McDonald RA. 1989. Nearshore water motion and mean flows in a multiple parallel bar system. *Marine Geology* **86**: 321-338.

Davidson-Arnott R. 2010. Introduction to Coastal Processes and Geomorphology. Cambridge University Press: New York.

De Bakker ATM, Tissier MFS, Ruessink BG. 2014. Shoreline dissipation of infragravity waves. *Continental Shelf Research* **72**: 73-82.

De Vries S, Hill DF, De Schipper MA, Stive MJF. 2011. Remote sensing of surf zone waves using stereo imaging. *Coastal Engineering* **58**: 239-250.

Elgar S, Raubenheimer B, Guza RT. 2001. Current Meter Performance in the Surf Zone. *Journal of Atmospheric and Oceanic Technology* **18**: 1735-1746.

Elgar S, Raubenheimer B, Guza RT. 2005. Quality control of acoustic Doppler velocimeter data in the surfzone. *Measurement Science and Technology* **16**: 1889-1893.

Feddersen F. 2010. Quality Controlling Surf Zone Acoustic Doppler Velocimeter Observations to Estimate the Turbulent Dissipation Rate. *Journal of Atmospheric and Oceanic Technology* **27**: 2039-2055.

Gaillard P, Gauthier M, Holly F. 1980. Method of analysis of random wave experiments with reflecting coastal structures. *Proceedings of the 17th International Conference on Coastal Engineering*, ASCE, 204-220.

Galvin CJ. 1968. Breaker type classification on three laboratory beaches. *Journal of Geophysical Research* **73**: 3651-3659.

Green MO. 1999. Test of sediment initial-motion theories using irregular-wave field data. *Sedimentology* **46**: 427-441.

Guedes RMC, Bryan KR, Coco G. 2013. Observations of wave energy fluxes and swash motions on a low-sloping, dissipative beach. *Journal of Geophysical Research* **118**: 3651-3669.

Guza RT, Thornton EB, Holman RA. 1984. Swash on steep and shallow beaches. *Proceedings of the 19th International Conference on Coastal Engineering*, ASCE, 708-723.

Guza RT, Thornton EB. 1985. Observations of Surf Beat. *Journal of Geophysical Research* **90**: 3161-3172.

Guza RT, Clifton MC, Rezvani F. 1988. Field Intercomparisons of Electromagnetic Current Meters. *Journal of Geophysical Research* **93**: 9302-9314.

Haller MC, Honegger D, Catalan PA. 2014. Rip Current Observations via Marine Radar. *Journal of Waterway, Port, Coastal and Ocean Engineering* **140**: 115-124.

Hegge BJ, Masselink G. 1996. Spectral Analysis of Geomorphic Time series: Auto-Spectrum. *Earth Surface Processes and Landforms* **21**: 1021-1040.

Holman RA, Symonds G, Thornton EB, Ranasinghe R. 2006. Rip spacing and persistence on an embayed beach. *Journal of Geophysical Research* **111**: C01006.

Holman RA, Stanley L. 2007. The history and technical capabilities of Argus. *Coastal Engineering* **54**: 477-491.

Holman RA, Haller MC. 2013. Remote Sensing of the Nearshore. *Annual Review of Marine Science* **5**: 95-113.

Huntley DA, Hendry MD, Haines J, Greenidge B. 1988. Waves and Rip Currents

on a Caribbean Pocket Beach, Jamaica. *Journal of Coastal Research* **4**: 69-79.

Jenkins GM, Watts DG. 1968. Spectral Analysis and its Applications. Holden-Day: San Francisco.

Johnson D, Pattiaratchi C. 2004. Application, modelling and validation of surfzone drifters. *Coastal Engineering* **51**: 455-471.

Komar PD. 1998. Beach Processes and Sedimentation: Second Edition. Prentice Hall: New Jersey.

Longuet-Higgins MS. 1952. On the statistical distribution of the height of sea waves. *Journal of Marine Research* **11**: 245-266.

MacMahan J, Brown J, Thornton E. 2009. Low-Cost Handheld Global Positioning System for Measuring Surf-Zone Currents. *Journal of Coastal Research* **25**: 744-754.

MacVicar BJ, Beaulieu E, Champagne V, Roy AG. 2007. Measuring water velocity in highly turbulent flows: field tests of an electromagnetic current meter (ECM) and an acoustic Doppler velocimeter (ADV). *Earth Surface Processes and Landforms* **32**: 1412-1432.

Masselink G. 1995. Group bound long waves as a source of infragravity energy in the surf zone. *Continental Shelf Research* **15**: 1525-1547.

Masselink G, Puleo JA. 2006. Swash-zone morphodynamics. *Continental Shelf Research* **26**: 661-680.

Masselink G, Hughes MG, Knight J. 2011. Coastal Processes and Geomorphology: Second Edition. Hodder Education: London.

McCarroll RJ, Brander RW, Turner IL, Power HE, Mortlock TR. 2014. Lagrangian observations of circulation on an embayed beach with headland rip currents. *Marine Geology* **355**: 173-188.

Morang A, Larson R, Gorman L. 1997. Monitoring the Coastal Environment; Part 1: Waves and Currents. *Journal of Coastal Research* **13**: 111-133.

Puleo JA, Faries JWC, Davidson M, Hicks B. 2010. A Conductivity Sensor for Nearbed Sediment Concentration Profiling. *Journal of Oceanic and Atmospheric Technology* **27**: 397-408.

Puleo JA, Lanckriet T, Wang P. 2012. Near bed cross-shore velocity profiles, bed shear stress and friction on the foreshore of a microtidal beach. *Coastal Engineering* **68**: 6-16.

Puleo JA, Lanckriet T, Blenkinsopp C. 2014. Bed level fluctuations in the inner surf and swash zone of a dissipative beach. *Marine Geology* **349**: 99-112.

Ridd PV. 1992. A sediment level sensor for erosion and siltation detection. *Estuarine, Coastal and Shelf Science* **35**: 353-362.

Rodriguez A, Sanchez-Arcilla A, Redondo JM, Mosso C. 1999. Macroturbulence measurements with electromagnetic and ultrasonic sensors: a comparison under high-turbulent flows. *Experiments in Fluids* **27**: 31-42.

Ruessink BG. 1999. Data report 2.5D experiment Egmond aan Zee. Department of Physical Geography, University of Utrecht, The Netherlands.

Ruessink BG, Bell PS, Van Enckevort IMJ, Aarninkhor SGJ. 2002. Nearshore bar crest location quantified from time-averaged X-band radar images. *Coastal Engineering* **45**: 19-32.

Russell PE. 1993. Mechanisms for beach erosion during storms. *Continental Shelf Research* **13**: 1243-1265.

Saulter AN, Russell PE, Gallagher EL, Miles, JR. 2003. Observations of bed level change in a saturated surf zone. *Journal of Geophysical Research* **108**: 3112.

Schmidt WE, Woodward BT, Millikan KS, Guza RT, Raubenheimer B, Elgar S. 2003. A GPS-Tracked Surf Zone Drifter. *Journal of Atmospheric and Oceanic Technology* **20**: 1069-1075.

Scott TM, Russell PE, Masselink G, Wooler A, Short AD. 2007. Beach Rescue Statistics and their Relation to Nearshore Morphology and Hazard: A Case Study for Southwest England. *Journal of Coastal Research* **SI 50**: 1-6.

Scott TM, Russell PE, Masselink G, Wooler A. 2008. High volume sediment transport and its implications for recreational beach risk. *Proceedings of the 31st International Conference on Coastal Engineering*, ASCE, 4250-4262.

Senechal N, Coco G, Bryan KR, Holman RA. 2011a. Wave runup during extreme storm

conditions. *Journal of Geophysical Research* **116**: C07032.

Senechal N, Abadie S, Gallagher E, MacMahan J, Masselink G, Michallet H, Reniers A, Ruessink G, Russell P, Sous D, Turner I, Ardhuin F, Bonneton P, Bujan S, Capo S, Certain R, Pedreros R, Garlan T. 2011b. The ECORS-Truc Vert'08 nearshore field experiment: presentation of a three-dimensional morphologic system in a macro-tidal environment during consecutive extreme storm conditions. *Ocean Dynamics* **61**: 2073-2098.

Sheremet A, Guza RT, Elgar S, Herbers THC. 2002. Observations of nearshore infragravity waves: Seaward and shoreward propagating components. *Journal of Geophysical Research* **107**: C8.

Short AD, Brander RW. 1999. Regional Variations in Rip Density. *Journal of Coastal Research* **15**: 813-822.

Suhayda JN. 1974. Standing waves on beaches. *Journal of Geophysical Research* **79**: 3065-3071.

Thornton EB, Guza RT. 1982. Energy saturation and phase speeds measured on a natural beach. *Journal of Geophysical Research* **87**: 9499-9508.

Thornton EB, Guza RT. 1983. Transformation of Wave Height Distribution. *Journal of Geophysical Research* **88**: 5925-5938.

Van Dongeren A, Battjes J, Janssean T, Van Noorloos J, Steenhauer K, Steenbergen G, Reniers A. 2007. Shoaling and shoreline dissipation of low-frequency waves. *Journal of Geophysical Research* **112**: C02011.

Woodroffe CD. 2002. Coasts: form, process and evolution. Cambridge University Press: Cambridge.